Composites Part C: Open Access 2 (2020) 100017

Contents lists available at ScienceDirect

Composites Part C: Open Access

journal homepage: www.elsevier.com/locate/jcomc

# Tensile and flexural properties of epoxy laminates with natural papaya bast fibre cellular layers

Gabriela Luiza Cota Coura [a], Rodrigo Teixeira Santos Freire [a,b,*], Júlio César dos Santos [a], Lívia Ávila de Oliveira [a,b], Fabrizio Scarpa [c], Túlio Hallak Panzera [a]

[a] Centre for Innovation and Technology in Composite Materials – CITeC, Department of Mechanical Engineering, Federal University of São João del Rei - UFSJ, 36307-344, Brazil
[b] Department of Natural Sciences – Federal University of São João del Rei – UFSJ, Brazil
[c] Bristol Composites Institute (ACCIS), University of Bristol, UK

ARTICLE INFO

*Keywords:*
Papaya bast fibre
Laminated composite
Honeycomb-like structure
Mechanical properties

ABSTRACT

This work focuses on the fabrication and characterisation of epoxy composites reinforced with natural fibre layers extracted from the inner bast (phloem) of the papaya plant (Carica papaya) under tensile and three-point bending loading. The papaya phloem is composed of fibrous laminas that wrap and reinforce the stem of the plant. A set of quasi-periodically arranged holes disrupt the continuity of these layers, through which the branches emerge. The fibres in each layer constitute an anisotropic honeycomb-like structure, whose elongated cells align along a single preferential direction. Papaya-reinforced epoxy composites are fabricated by hand lay-up and evaluated using two full-factorial designs based on the fibre-to-load direction in longitudinal (0°) and transverse (90°) conditions, for configurations without holes and alternating holes. Composites made with randomly-oriented short fibres are also evaluated along with the first experiment. The tensile and flexural properties obtained are compared to other materials in the literature to assess its potential as a structural material. The results show that the papaya bast fibre layers can be a promising reinforcement for polymeric composites.

## 1. Introduction

Sustainability and environmental issues have recently intensified the research on natural fibres in material science and engineering. This interest is justifiable since these fibres are biodegradable and obtained from renewable resources [1,2]. Natural fibres such as flax, hemp, jute, sisal, coir and henequen have been used since ancient times in a wide variety of products, from clothing to house roofing [3,4]. Papaya bast fibres, however, have been much less explored.

The papaya plant (Carica papaya) is widely cultivated in tropical and subtropical regions for its fruits, and Brazil is its second-largest world producer [5]. Carica papaya is considered a giant herb and does not contain wood (lignified xylem) as trees in general. However, despite its parenchymal, less resistant xylem, this species can reach up to 10 m in height [6], due to its high flexural modulus and strength provided by the fibre layers of the stem. Papaya fibres are, therefore, a potential reinforcement phase for polymeric composite materials [7,8].

Papaya fibres are potentially economically viable alternatives as well. Large extensions of arable land are necessary for the production of natural fibres for industry (e.g. cotton and sisal), competing with areas for food production. Plants like papaya do not pose this problem, as they produce both fruits and fibres. Papaya plantations are replaced every three to five years, and stems are usually discarded. However, the stems could be collected for the extraction of fibres, supplying a large amount of raw material, with an estimated total amount of 1.2 million tonnes for each replacement cycle [5–11]. The inner bast (phloem) of C. papaya is composed of fibrous layers, which surround and reinforce the stem of the plant. Each layer is a fibre mesh with an anisotropic, honeycomb-like structure, whose elongated cells align in a single preferred direction (see Fig. 7 in the Morphological Analysis section). These layers, which originate from a lamina of undifferentiated cells (vascular cambium), progressively migrate towards the outer surface of the stem as the plant grows and new inner layers are formed [6,9,10]. The most mature outer layer is sclerified (i.e., thickened and lignified) and

* Corresponding author at: Centre for Innovation and Technology in Composite Materials – CITeC, Department of Mechanical Engineering, Federal University of São João del Rei - UFSJ, 36307-344, Brazil.
*E-mail address:* rfreire@ufsj.edu.br (R.T.S. Freire).

https://doi.org/10.1016/j.jcomc.2020.100017
Received 2 July 2020; Received in revised form 3 August 2020; Accepted 3 August 2020

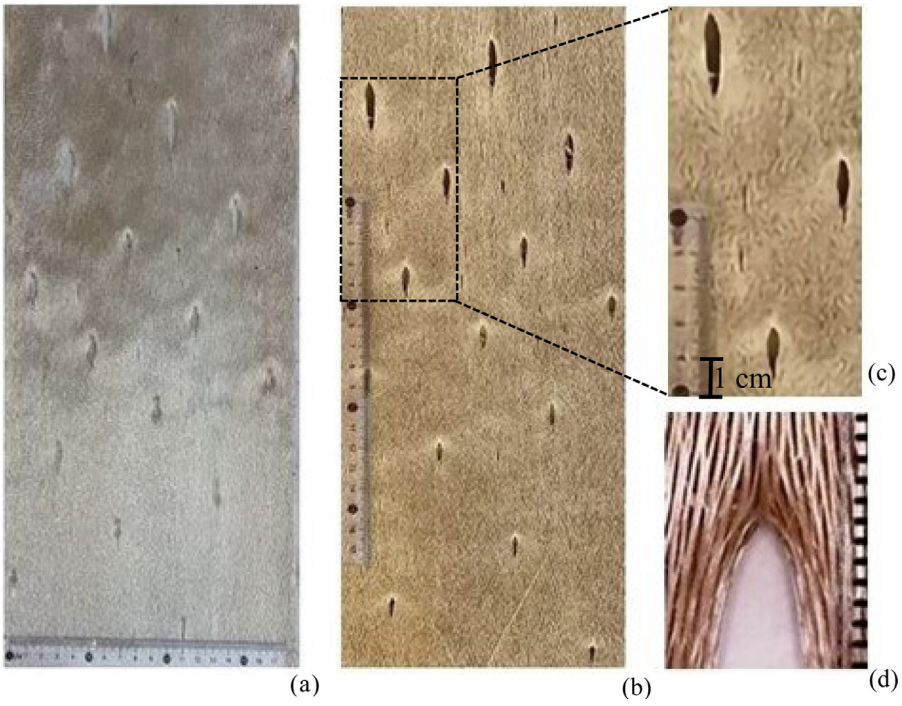


**Fig. 1.** Papaya bast fibre (a) inner and (b) intermediate layers; (c) magnification of the intermediate layer (selected region in (b)); (d) typical morphology of the edge of the holes (optical microscopy with a millimetric ruler).

**Table 1**
Chemical composition of C. papaya and other natural fibres (adapted from [8]).

| Fibre | Cellulose (%) | Hemicellulose (%) | Lignin (%) | Wax (%) | Ash (%) |
|---|---|---|---|---|---|
| C. Papaya | 58.71 | 11.8 | 14.26 | 0.81 | 4.7 |
| Coir | 43 | 1.7 | 45 | – | – |
| Bamboo | 26 | 31 | 30 | – | – |
| Jute | 72 | 13 | 13 | 0.5 | 0.5-2 |
| Flax | 81 | 14 | 3 | 1.7 | – |
| Ramie | 76 | 15 | 1 | – | – |
| Hemp | 74 | 18 | 4 | 2.3 | 1480 |
| Kenaf | 53.14 | 14.33 | 8.18 | 0.8 | 2-5 |
| Sisal | 60-78 | 10-14.2 | 8-14 | 2.0 | – |
| Cotton | 82.7 | 5.7 | – | – | – |

its extraction is difficult, since it is thinner and more fragile. The inner and intermediate layers are the ones therefore used in this work. More information about these layers is provided in the Material and Methods section. A set of quasi-periodically arranged holes is visible in the laminas (Fig. 1(a)–(c)). During the growth cycle of the plant, the branches emerge through these layers, after the fall of the older and more mature branches, and these perforations remain. The morphology of a single perforation is presented in Fig. 1 (d) in a close-up at the edge of the hole. Further information about the morphology of these holes is presented in the Results and Discussion section. These pictures were obtained from fibre layers extracted in this work.

Kumaar et al. [8] performed a thorough physicochemical characterization of Carica papaya fibres, summarised in Table 1. The cellulose content of C. papaya fibres, although lower than cotton, ramie, flax, hemp and jute, is comparable to sisal and higher than coir and kenaf, among others. It is worth noting that the chemical composition of natural fibres depends on the age of the plant, climate conditions, extraction methods and soil [8]. The FTIR analysis performed by Kumaar et al. revealed hydroxyl and carbonilic groups, as well as methyl and methylene groups present in cellulose and hemicellulose. Aromatic rings of lignin were also identified [8].

Kempe et al. [7] characterised papaya bast fibres and obtained tensile modulus and strength of up to 10 GPa and 100 MPa, respectively. Although these values are comparatively lower than those of natural fibres in general [12,13], the density of the papaya fibre is one of the lowest in the plant kingdom (approximately $0.86 \pm 0.07$ g/cm$^3$) [5,14], and this makes the specific properties of the fibre attractive to produce sustainable composite materials. Lautenschläger et al. [6] were probably the first to fabricate and evaluate the mechanical properties of composites reinforced with papaya bast fibres. Short papaya fibres (~ 10 mm) in polypropylene composites with a fibre volume fraction of 30% were investigated. The fibres were obtained from the maceration of the parenchymal tissue of the plant stem and subsequently cut. These authors observed an increase in the tensile modulus (strength) of up to 162% (26.4%) relative to the pure resin.

Kumaar et al. [15] have quite recently investigated the mechanical properties of epoxy laminates reinforced by alkali-treated continuous fibre layers of C. papaya. The laminates were fabricated by hand lay-up and compression moulding. Different fibre-matrix mass fractions (10, 20 and 30%) and orientations of the layers (0, 45 and 90°) were considered. Best tensile (122 MPa), flexural (118.9 MPa) and impact (7.8 J) strengths have been obtained for 20 wt% and fibres oriented at 0°, and the authors conclude that papaya bast fibre-reinforced composites are suitable for light-weight industrial applications.

Papaya bast fibres layers present a cellular configuration. Cellular (fractal) fibres extracted from the cactus O. ficus-indica have also been used as reinforcement in polyester composites, showing very high bending to axial stiffness ratios (up to 7) and high damping capacity under bending fatigue loading [9,10]. However – to the best of the authors' knowledge – the work presented in this paper represents the first at-

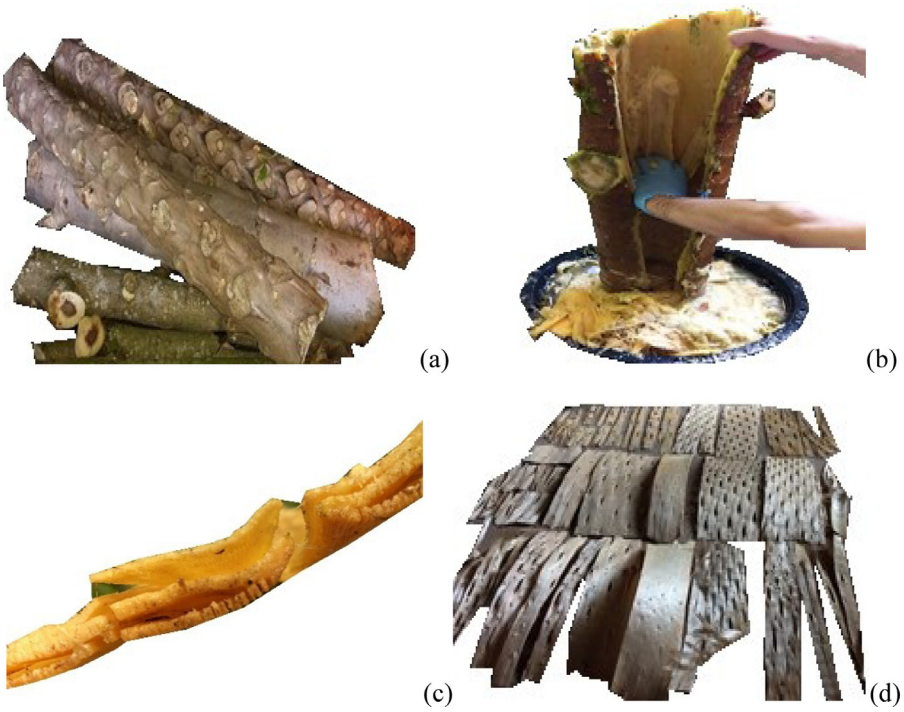


**Fig. 2.** (a) Carica papaya cut stems; (b) removal of the parenchymal xylem; (c) inner, intermediate and external fibre layers; (d) dried extracted layers

tempt to investigate epoxy composites reinforced with continuous papaya bast fibres considering different types of fibre layers as well as the holes, which spread all over the layers. Two full-factorial designs are carried out to evaluate the effects of the fibre layer and morphology on the tensile and flexural properties of composites reinforced with fibres oriented at 0° and 90° relative to the sample length.

## 2. Materials and methods

### 2.1. Materials

An epoxy system composed of RenLam M resin and Aradur HY96 hardener is used as a matrix phase, being supplied by Huntsman (Brazil). Bast fibres are extracted from papaya plants in the central-western region of the state of Minas Gerais (Brazil).

### 2.2. Fibre extraction

The extraction of papaya bast fibres follows the process described by Kumaar et al. [8]. The papaya stems (Fig. 2(a)) are cut and immersed in tap water at room temperature for 15 days, after which the inner core (parenchymatous xylem) can be manually removed and discarded (Fig. 2(b)). The remaining bark is again immersed in water and, after an additional 15 days, the fibre layers can be manually separated. The authors identified three distinct laminar regions, as shown in Fig. 2(c)). These layers are water cleansed and dried in the shade for a week (Fig. 2(d)). The process is eco-friendly, and no chemical or physical treatments are performed on the extracted fibres.

### 2.3. Statistical analysis

A full-factorial design ($2^1 3^1$) has been established to investigate the effect of the type of fibre used (internal and intermediate) and its morphology (without holes, alternating holes and randomly oriented short fibres (5–20 mm)) on the tensile and flexural properties of the laminates. The reinforcements on the composite beams were oriented along the sample length (0°). A second design ($2^2$) has been set up to investigate the same set of composites, this time with fibre layers transversely oriented to the sample length (90°), except for the condition with short fibres randomly oriented. The experimental conditions are presented in Table 2. The Minitab v.18 software has been used to analyse the data following Design of Experiment (DoE) and Analysis of Variance (ANOVA) techniques. The constant factors in the experiments are fibre grammage (0.15 g/cm$^2$) and uniaxial pressure level (654 kPa for 24 h, based on previous work [16]). The humidity level during manufacture ranges from 53% to 58%. Multiple layers can be stacked with coincident holes, or in such a way to cover the holes of subsequent layers in the final laminate (alternating holes). Six samples are fabricated (three for tensile and three for bending tests) for each experimental condition. Five replicates are considered totalling 180 and 120 samples for the first and second experiments, respectively.

**Table 2**
Full factorial designs: Experiment I ($2^1 3^1$) and Experiment II ($2^2$)

| Experimental Condition | Type of fibre (layer) | Morphology |
|---|---|---|
| Experiment I | | |
| I-No_0 | Inner | No holes |
| I-Alt_0 | Inner | Alternating holes |
| I-Rnd | Inner | Randomly oriented ground fibres |
| Int-No_0 | Intermediate | No holes |
| Int-Alt_0 | Intermediate | Alternating holes |
| Int-Rnd | Intermediate | Randomly oriented ground fibres |
| Experiment II | | |
| I-No_90 | Inner | No holes |
| I-Alt_90 | Inner | Alternating holes |
| Int-No_90 | Intermediate | No holes |
| Int-Alt_90 | Intermediate | Alternating holes |

### 2.4. Manufacturing process

The laminates are manufactured by hand lay-up at room temperature, followed by cold uniaxial compaction. Initially, the papaya fibre layers are cut (or ground, in case of short fibres) and assembled according to the morphology factor levels (Table 1). The fibres are cut using a knife mill, to a size of approximately 5–20 mm. The selected fibre grammage (fixed at 0.15 g/cm$^2$) determines the number of layers used.

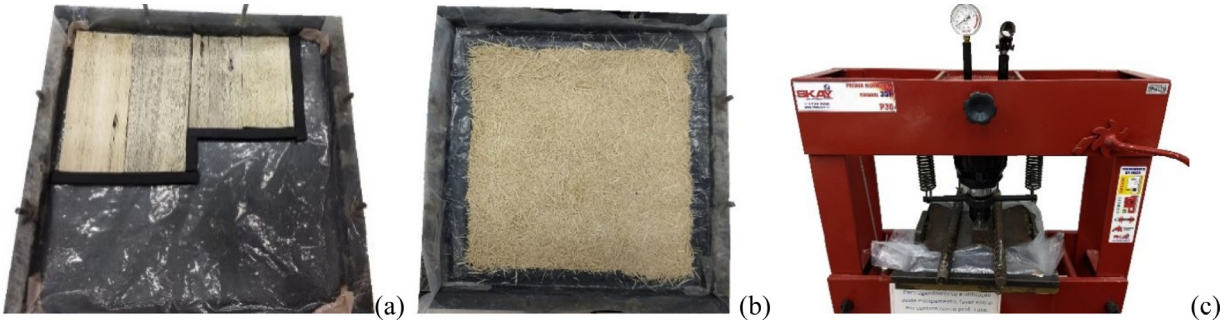

**Fig. 3.** Fabrication of the composites: papaya fibre layers (a) or randomly oriented short fibres (b) placed onto the metallic mould; (c) cold pressing.

**Fig. 4.** Samples with longitudinally-oriented fibre layers: (a) alternating holes, (b) no holes; (c) randomly oriented ground fibres; samples with transversely oriented fibre layers: (d) alternating holes, (e) no holes.

The fibre mass fraction ranges from 40% to 60%, corresponding to a fibre volume fraction of 46–66%. The fibre layers are pre-compacted at 20 MPa for 10 min before use. Preliminary experiments performed indicate that pre-compaction enhances the mechanical properties of the composites. The tensile modulus (strength) increases 68% (91%), while flexural modulus (strength) enhances 94% (120%). Each layer is laid one by one in a metallic mould (300 × 300 $mm^2$), pouring a sufficient amount of epoxy adhesive to ensure adequate wetting (Fig. 3a and b). The resin and hardener are mixed at the proportion of 5:1 (wt/wt), respectively, according to the manufacturer's recommendations. A plastic film is used inside the mould to provide a better surface finishing. A lid closes the mould and a pressure of 654 kPa is applied for 24 h, after which the material is demoulded and post-cured at 50 °C for 24 h following the manufacturer's recommendations. Finally, the samples are cut on a band saw in dimensions 165 × 19 × 3 $mm^3$ [17] and 114 × 15 × 3 $mm^3$ [18] for tensile and three-point bending (Fig. 4) tests, respectively, according to the ASTM standards.

### 2.5. Characterisation

#### 2.5.1. Morphological analysis

The structure of the inner, intermediate and external fibre layers are investigated using optical and scanning electronic microscopy (SEM), using a portable digital USB Jiusion and a Hitachi TM 3000 microscopes, respectively.

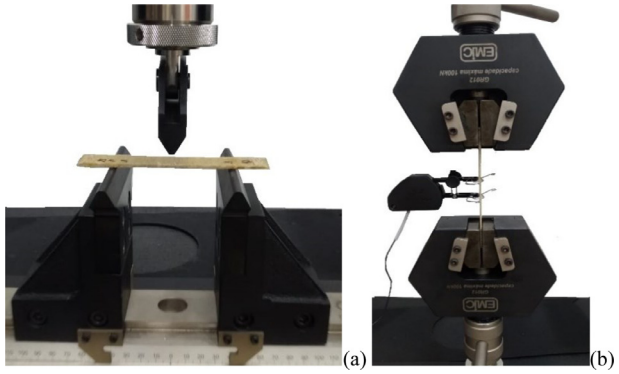

**Fig. 5.** Three-point bending (a) and tensile (b) tests.

#### 2.5.2. Mechanical characterisation

The three-point bending and tensile tests are performed based on the protocols of the ASTM D790-15 [17] and ASTM D638-14 [18] standards, respectively. An Instron 23100 universal testing machine, equipped with a 1 kN load cell, is used to perform the mechanical tests. The crosshead speed for both tests, obtained according to the standards, is 4 mm/min, with a span length of 96 mm for longitudinally oriented laminates and randomly oriented short fibres. For transversely oriented fibres, the crosshead speed is 2 mm/min, and, the span length (Fig. 5a) of the support, is 80 mm. A mechanical extensometer (Fig. 5b) was used to measure the tensile strain. The three-point bending deflection is obtained considering the translation of the crosshead.

## 3. Results and discussion

### 3.1. Morphological analysis

The extracted fibre layers are photographed and analysed using the ImageJ image processing software. The analysis performed on 43 fibre layers reveals that the holes (see Fig. 1) occupy up to 16% of the area of a sheet. The area occupied by each hole is also measured. Fig. 6 displays the frequency distribution of the size of these holes for the three types of layers obtained. It is worth noting that the size of the holes is considerable, reaching up to 32–34 $cm^2$, even though 90% of the holes are in the range of 0–16 $cm^2$, 0–10 $cm^2$ and 2–8 $cm^2$ for inner, intermediate and external layers, respectively.

The honeycomb-like structure of the fibre layers is analysed through optical microscopy (Fig. 7). Fig. 8 shows an illustration of the dimensional parameters of a unit cell of the honeycomb structure. The average dimensions of a unit cell are obtained analysing the images such as from

**Table 3**
Dimensional parameters of the unit cell.

| Type of fibre layer | Length (a) (mm) | Width (b) (mm) | Wall angle ($\theta$) (degrees) |
|---|---|---|---|
| Inner | 4.1 ± 1.1 | 0.43 ± 0.11 | 12.8° ± 3.5° |
| Intermediate | 3.3 ± 1.2 | 0.339 ± 0.076 | 14.2° ± 4.5° |
| External | 6.4 ± 1.4 | 0.36 ± 0.13 | 7.43° ± 3.01° |

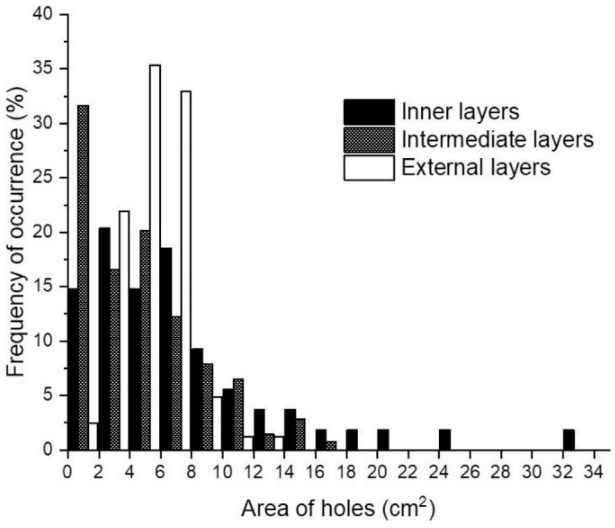


**Fig. 6.** Frequency distribution of the size of the holes for inner, intermediate and external layers. The numbers in the extremes of each triplet stand for the area range spanned by each group.

**Table 4**
Fibre density for each type of layer.

| Type of fibre | Density (g/cm$^3$) |
|---|---|
| Inner | 0.92 |
| Intermediate | 0.88 |
| External | 0.80 |

Fig. 7 using ImageJ and are presented in Table 3, considering a set of 25 measurements from different cells.

SEM analysis (Fig. 9) of the fibre bundles reveals the roughness of the surface, which is also increased by the presence of tyloses, i.e., pits in the fibre surface shown by the arrows (Fig. 9c). Such structures have also been described in other types of fibres as coir [19,20]. This roughness contributes to better fibre-matrix adhesion.

### 3.2. Fibre density

The fibre density is determined by water picnometry, according to ASTM D3800-99 [21]. The fibre density decreased towards the external layers (Table 4).

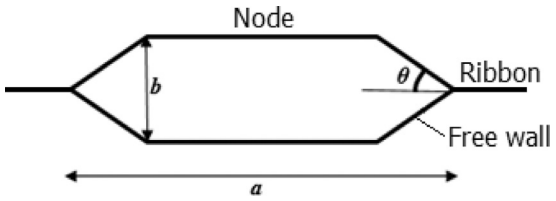


**Fig. 8.** Schematic drawing of a single cell of the honeycomb structure.

### 3.3. Mechanical tests

Tables 5 and 6 show the average values and the standard deviation of the mechanical responses obtained for longitudinally- (Experiment I) and transversely-oriented (Experiment II) laminates tested, considering five replicates. The following section will discuss the results of ANOVA obtained with these data. Figs. 10 and 11 present the typical tensile and flexural behaviour of the laminates, respectively, illustrated for longitudinally-oriented and randomly-oriented ground inner fibres. A massive reduction in stiffness and strength is observed between the honeycomb laminate and the short fibres. In contrast, similar stiffness is achieved by structures without and with alternated holes, the latter leading to reductions in maximum tensile stress (Fig. 10) and flexural load (Fig. 11).

### 3.4. Statistical analysis

Tables 7 and 8 show the Analysis of Variance (ANOVA) results obtained through Design of Experiments (DoE). The effect of different factors (or their interaction) is considered statistically significant for $P$-value $\leq 0.05$, that is, within a 95% confidence level (see underlined values). Values in bold are related to effects or interactions interpreted via effect plots. The $R^2$-adjusted values, ranging from 88.97% to 95.70% (Table 7) and 64.38% to 85.85% (Table 8), imply satisfactory predictability for the underlying statistical model used. P-values higher than 0.05 (0.088–0.853) obtained for the Anderson-Darling normality test indicate that the data follow a normal distribution, validating the statistical analysis. The Tukey's test is used to compare the levels of the factors for each effect plot. The same group of letters indicates statistically equivalent means, considering a 95% confidence interval.

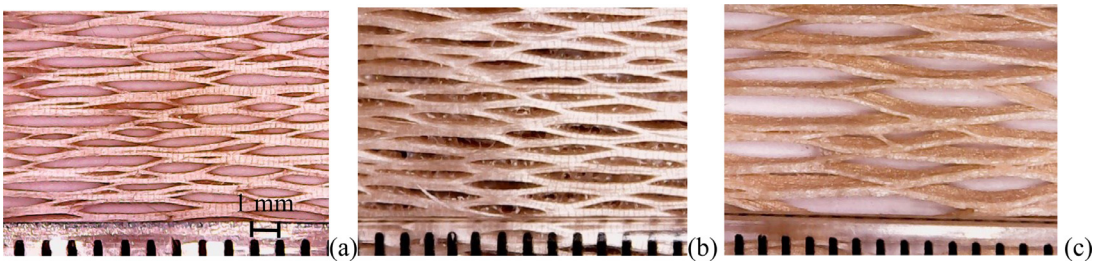


**Fig. 7.** Honeycomb-like structure of the fibre mesh: (a) inner (b) medium and (c) external layers.

**Table 5**
Descriptive statistics of composites containing longitudinal fibres (Experiment I).

| Experimental Condition | | Tensile Strength (MPa) | Modulus (GPa) | Flexural Strength (MPa) | Modulus (GPa) |
|---|---|---|---|---|---|
| Replicate 1 | I-NO_0 | 131.4 ± 7.8 | 14.53 ± 0.35 | 115 ± 11 | 13.4 ± 1.3 |
| | I-ALT_0 | 116 ± 11 | 12.3 ± 1.1 | 98 ± 25 | 11.4 ± 3.6 |
| | I-RND | 36.7 ± 3.4 | 5.27 ± 0.21 | 55.2 ± 5.7 | 4.01 ± 0.28 |
| | INT-NO_0 | 126 ± 28 | 17.8 ± 1.8 | 118.3 ± 6.0 | 12.21 ± 0.75 |
| | INT-ALT_0 | 78 ± 17 | 13.0 ± 2.7 | 109 ± 11 | 10.94 ± 0.63 |
| | INT-RND | 28.7 ± 1.9 | 5.9 ± 1.3 | 42.4 ± 7.4 | 3.34 ± 0.36 |
| Replicate 2 | I-NO_0 | 94 ± 15 | 13.11 ± 0.41 | 119 ± 11 | 13.57 ± 0.90 |
| | I-ALT_0 | 122 ± 11 | 14.20 ± 0.46 | 109 ± 13 | 12.65 ± 0.87 |
| | I-RND | 37.7 ± 2.9 | 4.99 ± 0.50 | 47.1 ± 4.9 | 3.68 ± 0.29 |
| | INT-NO_0 | 128 ± 18 | 17.66 ± 0.49 | 132 ± 12 | 14.1 ± 1.9 |
| | INT-ALT_0 | 99 ± 16 | 18.14 ± 0.90 | 106 ± 15 | 11.32 ± 0.96 |
| | INT-RND | 28.5 ± 1.8 | 4.51 ± 0.40 | 42.0 ± 6.1 | 3.14 ± 0.57 |
| Replicate 3 | I-NO_0 | 111.5 ± 8.9 | 13.4 ± 1.7 | 112 ± 19 | 11.9 ± 1.9 |
| | I-ALT_0 | 105 ± 19 | 12.9 ± 1.1 | 124 ± 15 | 13.0 ± 2.8 |
| | I-RND | 38.1 ± 2.5 | 4.87 ± 0.36 | 41.4 ± 4.1 | 3.56 ± 0.36 |
| | INT-NO_0 | 98 ± 10 | 12.52 ± 1.1 | 128 ± 20 | 13.1 ± 2.2 |
| | INT-ALT_0 | 80 ± 20 | 14.3 ± 2.1 | 107 ± 11 | 12.63 ± 1.2 |
| | INT-RND | 23.4 ± 2.7 | 4.57 ± 0.43 | 38.4 ± 3.9 | 2.95 ± 0.23 |
| Replicate 4 | I-NO_0 | 104 ± 10 | 13.0 ± 1.1 | 103.6 ± 6.2 | 11.91 ± 0.80 |
| | I-ALT_0 | 97.13 ± 9.7 | 13.7 ± 1.4 | 93 ± 11 | 9.7 ± 1.8 |
| | I-RND | 37.9 ± 1.2 | 4.64 ± 0.35 | 45.6 ± 4.1 | 3.32 ± 0.18 |
| | INT-NO_0 | 98 ± 20 | 12.32 ± 0.79 | 112 ± 12 | 12.9 ± 1.9 |
| | INT-ALT_0 | 88 ± 16 | 13.4 ± 2.1 | 106.7 ± 9.2 | 11.3 ± 1.8 |
| | INT-RND | 28.8 ± 7.0 | 4.46 ± 0.59 | 48.3 ± 6.5 | 3.50 ± 0.32 |
| Replicate 5 | I-NO_0 | 111 ± 21 | 14.26 ± 1.2 | 113.6 ± 2.2 | 12.63 ± 0.40 |
| | I-ALT_0 | 77.6 ± 6.0 | 10.1 ± 1.7 | 106.1 ± 5.5 | 10.57 ± 0.15 |
| | I-RND | 34.20 ± 0.65 | 4.64 ± 0.36 | 49.5 ± 3.8 | 3.47 ± 0.19 |
| | INT-NO_0 | 123 ± 18 | 15.3 ± 2.6 | 112 ± 38 | 10.9 ± 4.6 |
| | INT-ALT_0 | 91 ± 22 | 15.3 ± 3.8 | 110.1 ± 6.9 | 10.74 ± 0.61 |
| | INT-RND | 33.3 ± 2.0 | 4.83 ± 0.43 | 50.4 ± 2.1 | 3.63 ± 0.13 |

**Table 6**
Descriptive statistics of composites containing transverse fibres (Experiment II).

| Experimental Condition | | Tensile Strength (MPa) | Modulus (GPa) | Flexural Strength (MPa) | Modulus (GPa) |
|---|---|---|---|---|---|
| Replicate 1 | I-NO_90 | 1.9 ± 1.3 | 1.21 ± 0.13 | 2.7 ± 1.3 | 0.36 ± 0.22 |
| | I-ALT_90 | 1.06 ± 0.88 | 0.56 ± 0.16 | 2.3 ± 1.6 | 0.33 ± 0.21 |
| | INT-NO_90 | 1.59 ± 0.16 | 1.0 ± 1.1 | 4.8 ± 2.1 | 0.73 ± 0.62 |
| | INT-ALT_90 | 1.26 ± 0.95 | 0.77 ± 0.38 | 4.1 ± 2.6 | 0.47 ± 0.33 |
| Replicate 2 | I-NO_90 | 1.4 ± 1.5 | 1.26 ± 0.68 | 2.5 ± 1.2 | 0.41 ± 0.20 |
| | I-ALT_90 | 1.05 ± 0.66 | 0.67 ± 0.21 | 2.16 ± 0.62 | 0.34 ± 0.32 |
| | INT-NO_90 | 1.8 ± 1.4 | 1.16 ± 0.13 | 5.2 ± 2.2 | 0.60 ± 0.33 |
| | INT-ALT_90 | 1.2 ± 1.4 | 0.83 ± 0.31 | 3.7 ± 1.9 | 0.33 ± 0.09 |
| Replicate 3 | I-NO_90 | 1.58 ± 0.76 | 1.17 ± 0.34 | 3.8 ± 1.1 | 0.53 ± 0.12 |
| | I-ALT_90 | 0.76 ± 0.36 | 0.95 ± 0.38 | 2.50 ± 0.74 | 0.34 ± 0.15 |
| | INT-NO_90 | 1.72 ± 0.56 | 0.84 ± 0.43 | 5.2 ± 2.1 | 0.64 ± 0.10 |
| | INT-ALT_90 | 0.78 ± 0.35 | 0.75 ± 0.25 | 3.3 ± 3.7 | 0.47 ± 0.38 |
| Replicate 4 | I-NO_90 | 1.3 ± 1.2 | 1.46 ± 0.54 | 3.5 ± 1.6 | 0.50 ± 0.23 |
| | I-ALT_90 | 1.08 ± 0.61 | 0.89 ± 0.33 | 3.0 ± 3.1 | 0.47 ± 0.21 |
| | INT-NO_90 | 1.5 ± 1.7 | 1.00 ± 0.24 | 4.7 ± 3.7 | 0.82 ± 0.09 |
| | INT-ALT_90 | 0.96 ± 1.01 | 0.72 ± 0.34 | 3.9 ± 2.9 | 0.42 ± 0.44 |
| Replicate 5 | I-NO_90 | 1.6 ± 0.6 | 1.12 ± 0.09 | 3.6 ± 2.3 | 0.52 ± 0.29 |
| | I-ALT_90 | 0.91 ± 0.68 | 0.52 ± 0.11 | 2.10 ± 0.52 | 0.42 ± 0.41 |
| | INT-NO_90 | 1.28 ± 0.98 | 1.08 ± 0.40 | 4.99 ± 2.06 | 0.67 ± 0.43 |
| | INT-ALT_90 | 1.15 ± 0.62 | 0.80 ± 0.21 | 4.0 ± 2.4 | 0.63 ± 0.64 |

**Table 7**
ANOVA - Experiment I.

| | Experimental Factors | P-value ≤ 0.05 Tensile Strength (MPa) | Tensile Modulus (GPa) | Flexural Strength (MPa) | Flexural Modulus (GPa) |
|---|---|---|---|---|---|
| Main | Type of fibre (T) | 0.060 | 0.068 | 0.462 | 0.635 |
| Factors | Morphology (M) | **0.000** | **0.000** | **0.000** | **0.000** |
| Interaction | T x M | 0.297 | 0.294 | 0.249 | 0.952 |
| | $R^2$ - adj | 90.99% | 88.97% | 95.08% | 95.70% |
| P-value (Anderson Darling) ≥ 0.05 | | 0.355 | 0.088 | 0.454 | 0.231 |

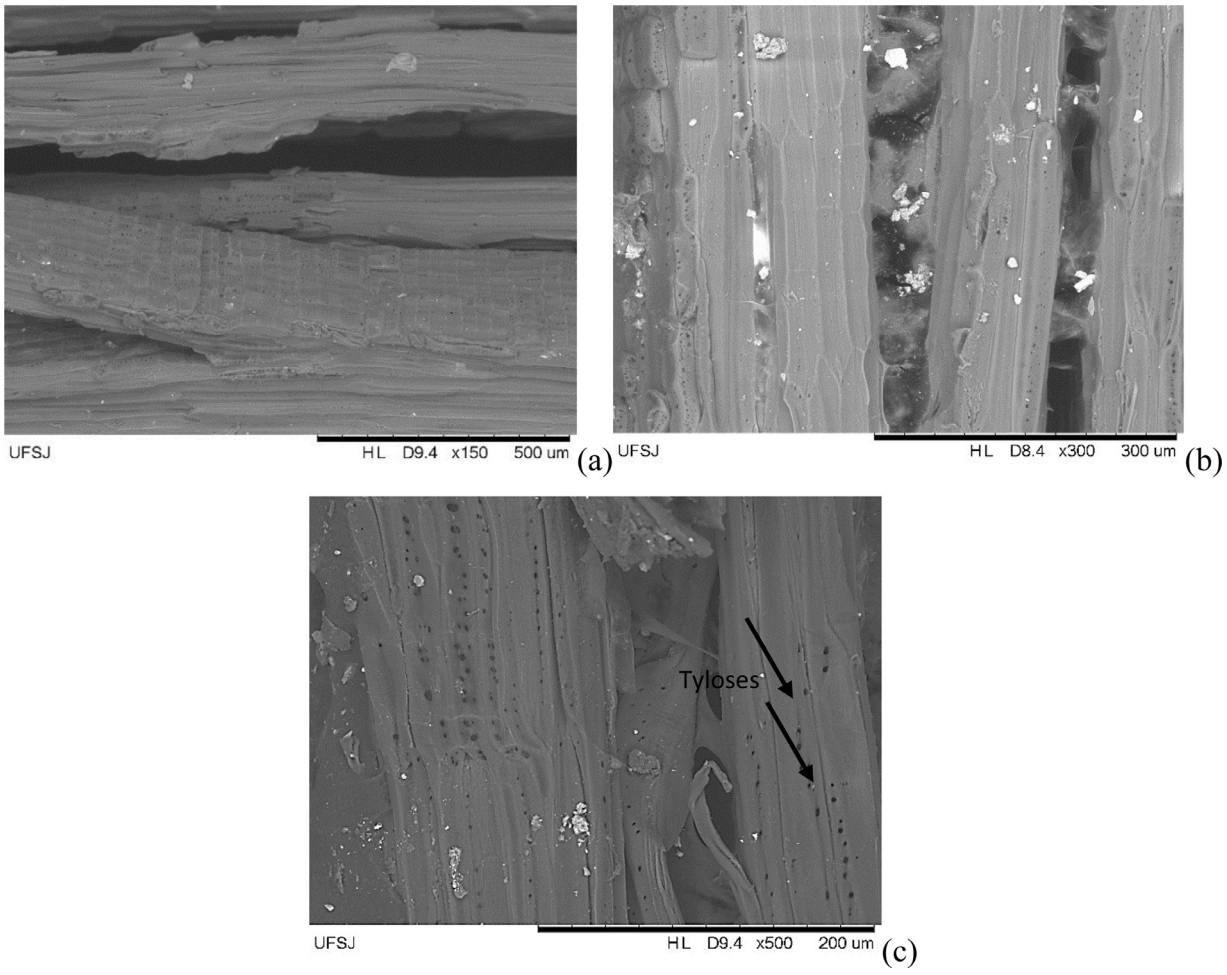


**Fig. 9.** SEM analysis of the surface of papaya fibres at (a) × 150 (b) × 300 (c) × 500.

**Table 8**
ANOVA - Experiment II.

| | Experimental Factors | P-value ≤ 0.05<br>Tensile Strength (MPa) | Tensile Modulus (GPa) | Flexural Strength (MPa) | Flexural Modulus (GPa) |
|---|---|---|---|---|---|
| Main | Type of fibre (T) | 0.569 | 0.160 | **0.000** | **0.001** |
| Factors | Morphology (M) | **0.000** | 0.000 | **0.000** | **0.001** |
| Interaction | T x M | 0.582 | **0.028** | 0.322 | 0.067 |
| | $R^2$ - adj | 67.08% | 70.61% | 85.85% | 64.38% |
| P-value (Anderson Darling) ≥ 0.05 | | 0.404 | 0.439 | 0.853 | 0.725 |

### 3.5. Experiment I: longitudinal fibre composites

Fig. 12 shows the main effect plots for the mean tensile strength (a) and modulus (b) for composites reinforced with longitudinally-oriented fibres. Composites reinforced with fibre layers without holes provide higher tensile strength and modulus. Laminates reinforced with fibre layers with alternating holes reveal reductions of 4.8% in tensile elastic modulus and 15.8% in tensile strength, which may be attributed to the concentration of stresses around the holes. The flexural properties show similar behaviour, with 8.36% reductions in flexural strength (Fig. 13a) and 9.94% in flexural modulus (Fig. 13b). In contrast, a substantial decrease (60-70%) in the tensile (Fig. 12) and flexural (Fig. 13) properties are observed for short fibres randomly oriented, since only a fraction of the fibres is oriented in the direction of loading.

It is worth noting, however, that the mean tensile modulus provided by layers with alternating holes is equivalent to that obtained for layers without holes, i.e., the reduction of 4.8% is not statistically significant according to Tukey´s test (Group A, Fig. 12b). This fact is important since the holes are distributed over the surface of the fibre layers, and layers without holes are much more difficult to produce. As previously discussed, perforations of considerable size occupy up to 16% of the area of a sheet. The removal of such holes is not practical and not profitable from an industrial point of view, as it will lead to a more complex and costlier manufacturing process. Large areas of the layers would be discarded. Moreover, the manufacturer would obtain an extensive collection of layer patches of different sizes, and the patchwork necessary to join them would lead to a large set of discontinuities, affecting the mechanical properties of the final composite laminates. The decrease in tensile strength (15.8%,), flexural strength (8.36%) and modulus (9.9%) were, by their turn, statistically significant.

### 3.6. Experiment II: transverse fibre composites

Fig. 14a presents the main effect of the morphological factor on the tensile strength of composites with transverse fibres. The tensile strength

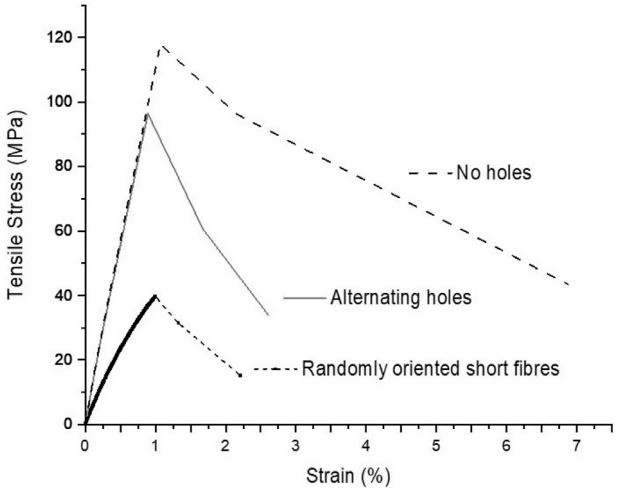


**Fig. 10.** Typical stress-strain behaviour of epoxy composites reinforced by longitudinally oriented or random short inner fibres.

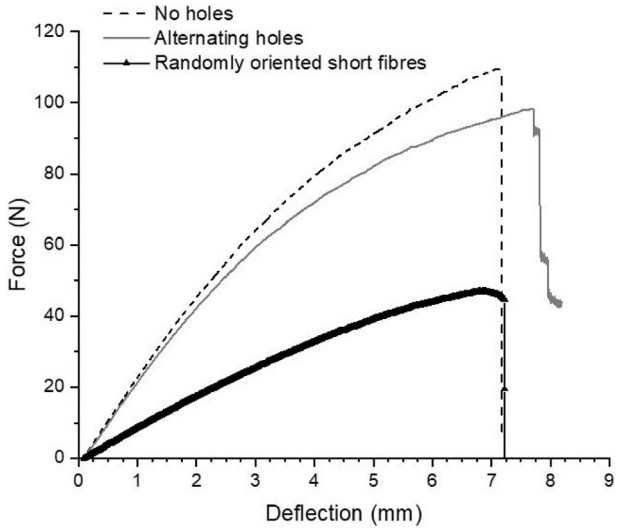


**Fig. 11.** Typical load-deflection behaviour of epoxy composites reinforced by longitudinally oriented or random short inner fibres.

is significantly higher (35.3%) for composites without holes, which may be explained by the stress concentration caused by the holes. The tensile modulus is also lower for composites with alternated holes, as shown in the fibre type-morphology interaction effect plot (Fig. 14b). Tensile stiffness and strength in the transverse fibre direction are much lower than for longitudinal composites since they are dominated by the properties of the matrix phase, as reported for different types of fibres, such as carbon, glass and flax fibres [22–24]. It is noteworthy, however, that the mean tensile modulus of samples with internal fibres is 18.5% higher relative to the one featured in specimens with intermediate fibres. This behaviour is evident only for layers with no holes. A small increase (7.28%) in tensile modulus for composites reinforced by layers with alternating holes is not significant, as indicated by Tukey's test, sharing the same group letter (C).

Fig. 15a shows the main effect plots for the fibre type and morphological factors on the flexural strength of composites made with transverse fibres (90°). The flexural strength is 36% lower for laminates with internal fibres compared to composites of intermediate fibre layers. Moreover, composites with alternating hole layers lead to a 24.40% reduction in flexural strength relative to those made without holes as expected, due to the high stress concentration generated by the holes. Fig. 15b reveals a similar behaviour for the flexural modulus, even though reductions are smaller (approx. 9%). The better performance of intermediate fibre layers might be related to their higher degree of sclerification (higher thickness and lignification of the fibres), which could improve their compressive modulus and strength. This hypothesis has yet to be verified. It is worth noting, however, that the tensile and flexural properties of the composites in the transverse direction are remarkably lower relative to those reinforced with longitudinal fibres.

### 3.7. Microstructural analysis

Fig. 16 shows the fractured region, obtained by optical microscopy, of a longitudinally reinforced composite with alternating holes submitted to a tensile test. Fig. 17 presents the cross-section of this region, investigated by scanning electron microscopy. Cracks propagate ortho- and diagonally to the load direction (see the left image of Fig. 16). The fractures occur in the node (green arrow), ribbon (blue arrow) and the free wall (red arrow) of the cell, as shown in the right image of Fig. 16.

The SEM images shown in Fig. 17 imply an efficient fibre-matrix adhesion, with little fibre pull-out and a fragile fracture mode. It is also worth noting the porous structure of the fibre bundles, which contributes to the reduced density of papaya fibres.

Fig. 18 presents the fractured surface of the laminates reinforced by transverse fibres under tensile load. The brittle fracture of the epoxy resin and the transverse fraying of the fibres are apparent.

### 3.8. Comparison of materials

The tensile and flexural properties of the papaya fibre-reinforced composites are compared to those of flax- [22] and glass fibre-reinforced [24] unidirectional laminates and with aluminium ISO 1200 [25], the latter being a common-choice for secondary structural applications

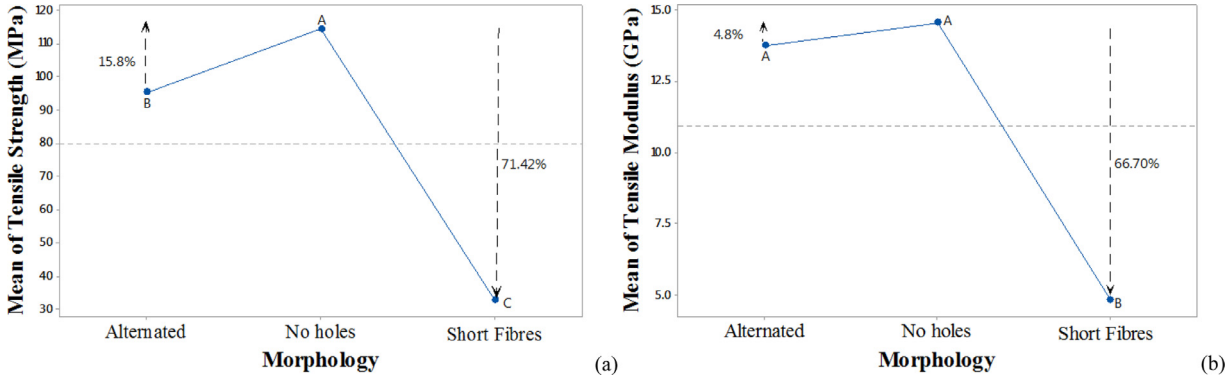


**Fig. 12.** Main effect plots for the mean of (a) tensile strength and (b) modulus of composites with longitudinal orientation.

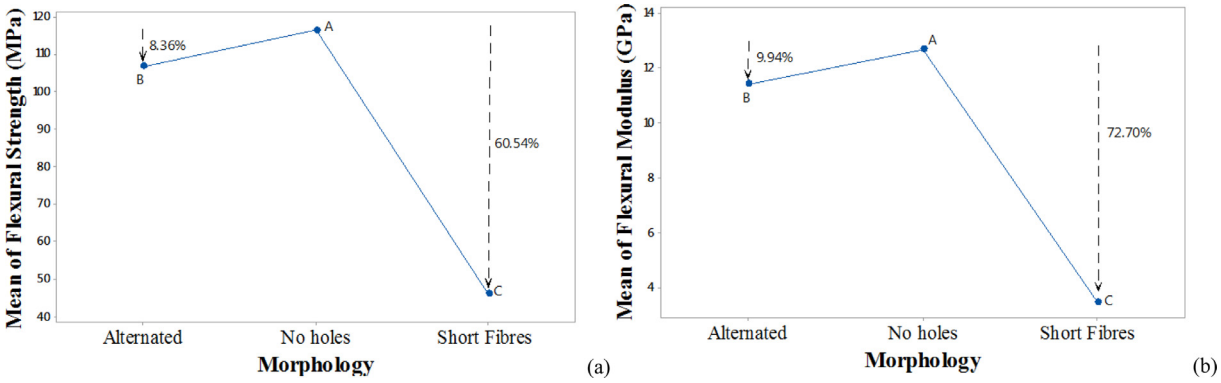


**Fig. 13.** Main effect plots for the mean (a) flexural strength and (b) modulus of composites with longitudinal orientation.

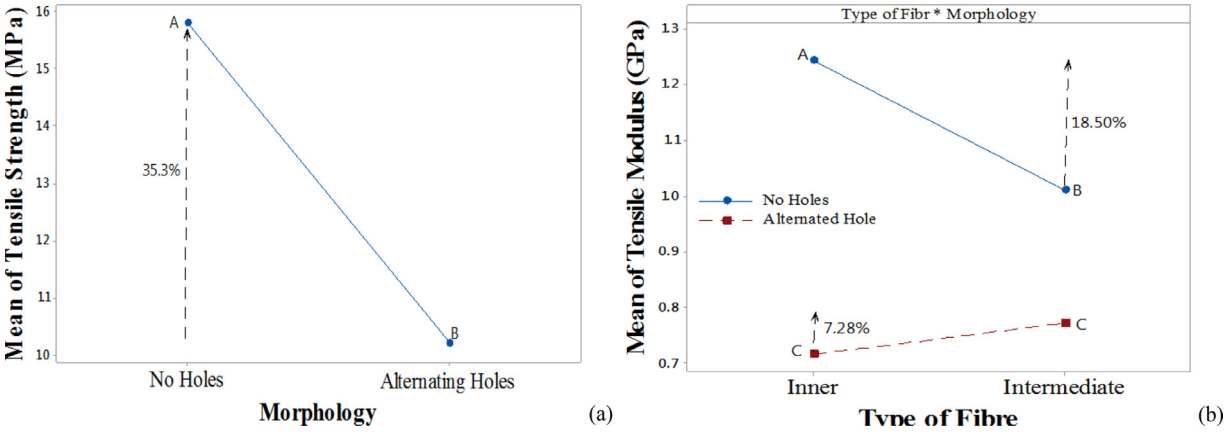


**Fig. 14.** (a) Main effect plot for the mean tensile strength and (b) interaction effect for the mean tensile modulus of composites with transverse orientation.

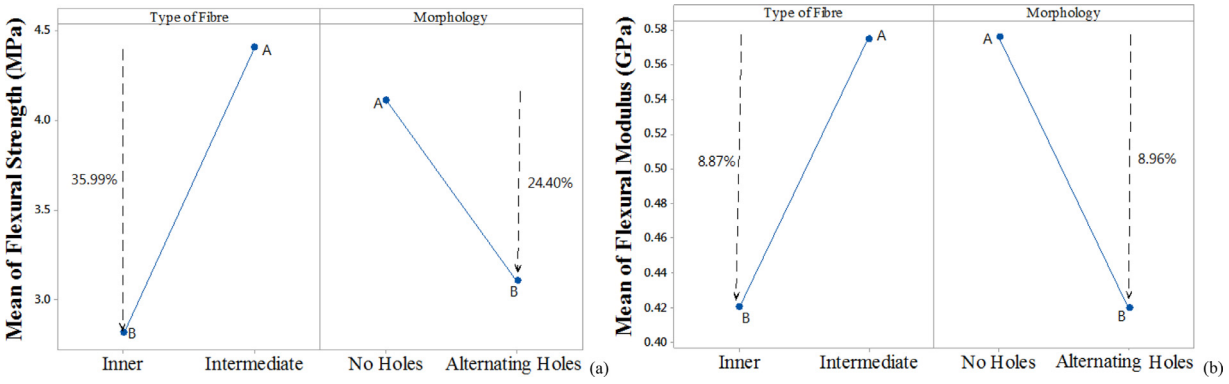


**Fig. 15.** Main effect plots for the mean (a) flexural strength and (b) modulus of composites with transverse orientation.

(Table 9). The papaya laminates used for comparison are those fabricated with alternating holes and longitudinally-oriented layer fibres. This choice is related to the higher availability of papaya fibre layers with holes and their high mechanical performance in the longitudinal direction. Compared to aluminium, the tensile (flexural) strength of the selected papaya laminates is 38% (55%) higher, although their tensile and flexural moduli are approximately 85% lower. The tensile and flexural strengths of papaya composites are only 10% of the respective value for epoxy glass composites, while the tensile and flexural moduli are approximately one-third. Synthetic glass fibres are, in fact, one of the strongest and stiffest fibres. Relative to the UD epoxy flax composites, the tensile strength and modulus of papaya composites are respectively 30% and 50% lower, as well as the flexural strength and modulus are respectively 50% and 36% lower. The cactus (O. ficus-indica) also presents cellular fibre layers similar to the ones extracted from C. papaya. Compared to cactus fibre-reinforced polyester composites [9], papaya fibre-reinforced composites provide substantially higher tensile and flexural modulus and strength. However, it important to point out that polyester presents lower tensile modulus and strength relative to epoxy (see Table 9).

It noteworthy that the results obtained in this work corroborate those reported by Kumaar et al. [15], who reported 122 MPa and 118.9 MPa for the tensile and flexural strength of epoxy composites reinforced by alkali-treated, longitudinally oriented layers (0°) with 20% of fibre mass fraction (see Table 9). In this work, the tensile (and flexural) strength obtained is, on average, 115 MPa. It is worth noting that these values correspond to the condition with no holes. Moreover, the fibre mass fraction used in the present work is higher, although no treatment is

**Table 9**
Comparison of papaya-epoxy mechanical properties and selected materials.

| Material | Fibre volume fraction (%) | Tensile Strength (MPa) | Modulus (GPa) | Flexural Strength (MPa) | Modulus (GPa) |
|---|---|---|---|---|---|
| Papaya reinforced composite (alternating holes, this study) | 46-66 | 95.47 | 13.74 | 106.9 | 11.42 |
| Aluminium (ISO 1200) | - | 69 | 70-105 | 69 | 70-105 |
| Epoxy glass fibre composites | 64 | 965 | 39.3 | 1150 | 38.6 |
| Epoxy flax fibre composites | 43-56 | 300.5 | 35.6 | 332.09 | 24.56 |
| Cactus fibre-polyester | 25 wt% | 15.8 | 1.48 | 66.50 | 7.95 |
| Papaya reinforced composite (no holes, [15]) | 20 wt% | 122 | NA* | 118.9 | NA* |

* Not Available in the cited reference.

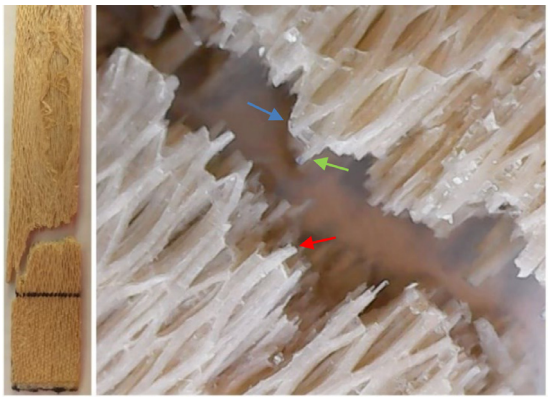

**Fig. 16.** Optical analysis of a fracture of longitudinally oriented fibre layer composite.

performed on the fibres. Alternating holes statistically significantly reduce the tensile strength (in 16%), and flexural modulus (in 10%) and strength (in 8.4%). The tensile modulus, however, is not statistically significantly affected by alternating holes. These findings are important, since, as previously discussed, holes are distributed all over the fibre layers, and their removal is not practical and not profitable from an industrial point of view, as it will lead to a more complex and costlier manufacturing process.

Papaya bast fibres, however, possess one of the lowest densities in the plant kingdom [7] (0.86 g/cm$^3$ versus 1.16 g/cm$^3$ for flax fibres [22]). Therefore, it is worth comparing specific mechanical properties in Table 10. The bulk density of papaya-epoxy composites was obtained in this work (1.0–1.5 g/cm$^3$), and aluminium (2.71 g/cm$^3$), UD glass fibre-reinforced laminates (1.85 g/cm$^3$) and UD epoxy flax fibre-reinforced laminates (1.26 g/cm$^3$) have been obtained in the literature [22–26]. The specific properties (or densities) of the papaya composites is not available in [15] for comparison.

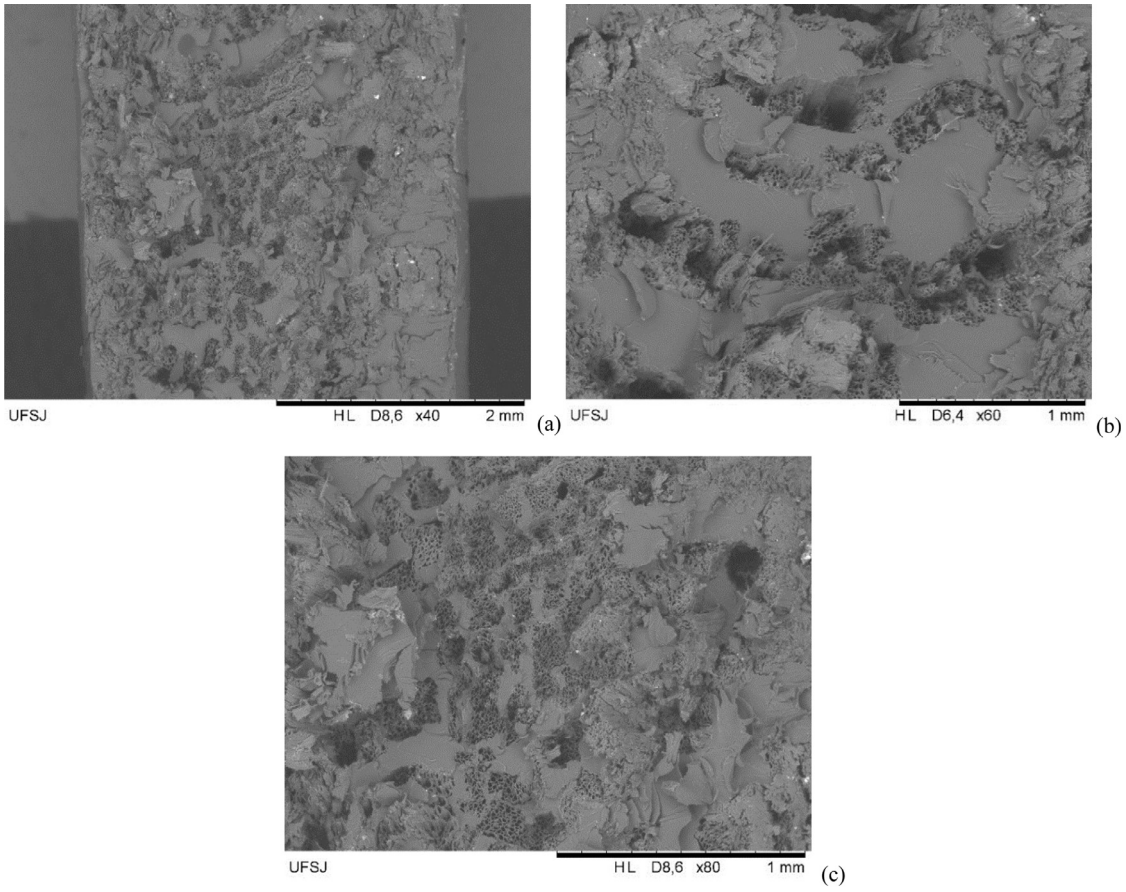


**Fig. 17.** SEM analysis of the fractured surface of longitudinal fibre-reinforced composites after the tensile test at (a) × 40 (b) × 60 and (c) × 80.

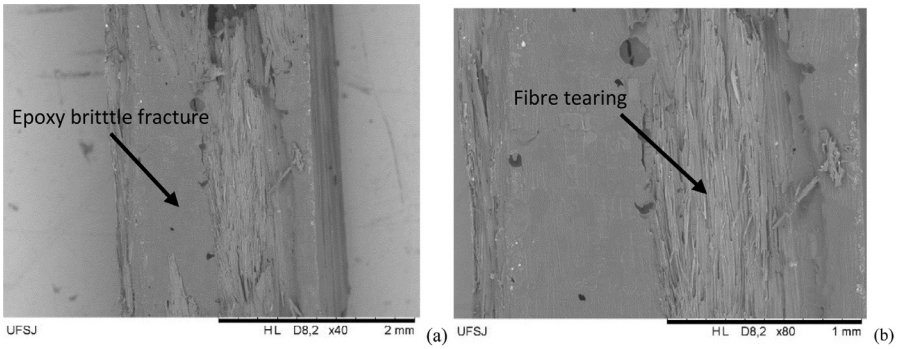


**Fig. 18.** The fractured surface of the transverse fibre-reinforced composites after the tensile test at (a) × 40 and (b) × 80.

**Table 10**
Comparison of papaya-epoxy mechanical specific properties and selected materials.

| Material | Density ($g/cm^3$) | Specific Tensile Strength ($N•m•g^{-1}$) | Modulus ($kN•m•g^{-1}$) | Specific Flexural Strength ($N•m•g^{-1}$) | Modulus ($kN•m•g^{-1}$) |
|---|---|---|---|---|---|
| Papaya reinforced composite (alternating holes) | 1.0-1.5 | 63.65 - 95.47 | 9.16 - 13.74 | 71.27 - 106.90 | 7.61 - 11.42 |
| Aluminium (ISO 1200) | 2.71 | 25.92 – 38.89 | 25.56 | 25.92 – 38.89 | 25.56 |
| Epoxy glass fibre composites | 1.85 | 521.62 | 21.24 | 621.62 | 20.86 |
| Epoxy flax fibre composites | 1.26 | 238.5 | 28.3 | 263.6 | 19.5 |

The specific tensile and flexural strengths of papaya-epoxy composites, although much lower (up to 86%) compared to epoxy glass fibre composites, are 145% and 175%, respectively higher relative to aluminium ISO 1200. The specific tensile and flexural moduli of papaya composites are approximately 50% of the respective values for aluminium or glass fibre composites. The specific tensile (flexural) strength of papaya composites is 22% (47%) less, and the specific tensile (flexural) modulus is 47% (30%) less compared to composites reinforced flax fibres. This comparison reveals that papaya bast fibre layers are a promising reinforcement for polymeric composites.

## 4. Conclusions

Epoxy composites reinforced with papaya bast fibres were characterised mechanically. The main findings are described below:

1 Laminates fabricated with longitudinally-oriented bast fibre layers without holes provide superior mechanical properties, achieving an average tensile strength of 115 MPa and flexural strength (modulus) of 115 MPa (12.7 GPa). Longitudinally-oriented laminates made with alternating holes provide similar mechanical performance with tensile strength of 95.47 MPa and flexural strength (modulus) of 106.9 MPa (11.42 GPa).
2 The mean tensile modulus provided by layers with alternating holes (13.74 GPa) is equivalent to that obtained for layers without holes (14.4 GPa), i.e., there is no statistically significant difference between these values according to Tukey´s test. This finding is important since the holes are ubiquitous across the papaya fibre layer surface. The selection of large regions without holes is difficult and would lead to the disposal of most of the material, as previously discussed.
3 The laminates that showed the best mechanical performance, in both directions analysed, are those without holes, which lead to stress concentrations.
4 Papaya bast fibre layers are highly anisotropic. The mechanical reinforcement performance of layers subjected to longitudinal loads, that is, along the longest axis of the honeycomb-like cells, is much superior relative to the transverse direction.
5 The tensile and flexural properties of epoxy composites reinforced by longitudinal papaya bast fibre layers with alternating holes are compared to those of different materials, leading to the conclusion that papaya bast fibre layers are a promising reinforcement for polymeric composites.

## Declaration of Competing Interest

The authors declare no conflicts of interest.

## Data for reference

The raw/processed data required to reproduce these findings cannot be shared at this time as the data also forms part of an ongoing study.

## Acknowledgements

The authors acknowledge the Brazilian Research Agencies, FAPEMIG (MSc scholarship) and CNPq (PQ - 309885/2019-1) for the financial support provided.

## References

[1] K.G. Satyanarayana, K. Sukumaran, P.S. Mukherjee, C. Pavithran, S.G.K. Pillai, Natural fibre-polymer composites, Cem. Concrete Comput. 12 (1990) 117–136.
[2] L. Yan, S. Su, N. Chouw, Microstructure, flexural properties and durability of coir fibre reinforced concrete beams externally strengthened with flax FRP composites, Compos. Part. B. 80 (2015) 343–354 https://doi.org/10.1016/j.compositesb.2015.06.011.
[3] M. Ramesh, K. Palanikumar, K.H. Reddy, Plant fibre based bio-composites: sustainable and renewable green materials, Renew. Sust. Energy Rev. 79 (2017) 558–584 https://doi.org/10.1016/j.rser.2017.05.094.
[4] H.P.S. Abdul Khalil, A.H. Bhat, A.F. Ireana Yusra, Green composites from sustainable cellulose nanofibrils: a review, Carbohydr. Polym. 87 (2012) 963–979 http://dx.doi.org/10.1016/j.carbpol.2011.08.078.
[5] E.A. Evans, F.H. Ballen, An Overview of Global Papaya Production, Trade, and Consumption, FE913, University of Florida, 2012.
[6] A. Kempe, T. Lautenschläger, A. Lange, C. Neinhuis, How to become a tree without wood- Biomechanical analysis of the stem of Carica papaya L, Plant Biol. 16 (1) (2014) 264–271 https://doi.org/10.1111/plb.12035.
[7] A. Kempe, A. Göhre, T. Lautenschläger, A. Rudolf, M. Eder, C. Neinhuis, Evaluation of bast fibres of the stem of Carica papaya L. for application as reinforcing material in green composites, Res. Rev. Biol. 6 (4) (2015) 245–252 https://doi.org/10.9734/ARRB/2015/15407.
[8] A. Saravana Kumaar, A. Senthilkumar, T. Sornakumar, S.S. Saravanakumar, V.P. Arthanariesewaran, Physicochemical properties of new cellulosic fibre extracted from Carica papaya bark, J. Nat. Fibres 16 (2) (2019) 175–184 https://doi.org/10.1080/15440478.2017.1410514.
[9] M. Bouakba, A. Bezazi, K. Boba, F. Scarpa, S. Bellamy, Cactus fibre/polyester biocomposites: manufacturing, quasi-static mechanical and fatigue characterization, Compos. Sci. Technol. 74 (2013) 150–159 http://dx.doi.org/10.1016/j.compscitech.2012.10.009.

[10] I. Zampetakis, Y. Dobah, A. Perriman, A. Hetherington, F. Scarpa, A. Bezazi, Meta–compliance and energy dissipation in cactus-based solids for defence and bone tissue engineering applications, in: Proceedings of the 20th International Conference on Composite Structures, 275, 2017.
[11] T. Lautenschläger, A. Kempe, C. Nienhuis, A. Wagenführ, S. Siwek, Not only delicious: papaya bast fibres in biocomposites, BioResources 11 (3) (2016) 6582–6589 https://doi.org/10.15376/biores.11.3.6582-6589.
[12] L.G. Thygesen, M. Eder, I. Burgert, Dislocations in single hemp fibres – investigations into the relationship of structural distortions and tensile properties at the cell wall level, J. Mater. Sci. 42 (2007) 558–564 https://doi.org/10.1007/s10853-006-1113-5.
[13] T. Gurunathan, S. Mohanty, S.K. Nayak, A review of the recent developments in biocomposites based on natural fibres and their application perspectives, Composites 77 (2015) 1–25 https://doi.org/10.1016/j.compositesa.2015.06.007.
[14] A.K. Bledzki, W. Zhang, A. Chate, Natural-fibre-reinforced polyurethane microfoams, Compos. Sci. Technol. 61 (16) (2001) 2405–2411 https://doi.org/10.1016/S0266-3538(01)00129-4.
[15] A. Saravana Kumaar, A. Senthilkumar, S.S. Saravanakumar, P. Senthamaraikannan, L. Loganathan, B. Muthu Chozha Rajan, Mechanical properties of alkali-treated carica papaya fiber-reinforced epoxy composites, J. Nat. Fibers (2020) https://doi.org/10.1080/15440478.2020.1739590.
[16] L.A. Oliveira, J.C. Santos, T.H. Panzera, R.T. Freire, L.M.G. Vieira, F. Scarpa, Evaluation of hybrid-short-coir-fibre-reinforced composites via full factorial design, Compos. Struct. (2018) https://doi.org/10.1016/j.compstruct.2018.01.088.
[17] ASTM D790-15e2, Standard Test Methods for Flexural Properties of Unreinforced and Reinforced Plastics and Electrical Insulating Materials, ASTM International, West Conshohocken, PA, 2015 https://www.astm.org/.
[18] ASTM D638-14, Standard Test Method for Tensile Properties of Plastics, ASTM International, West Conshohocken, PA, 2014 https://www.astm.org/.
[19] T.H. Nam, S. Ogihara, N.H. Tung, S. Kobayashi, Effect of alkali treatment on interfacial and mechanical properties of coir fiber reinforced poly(butylene succinate) biodegradable composites, Compos. Part B 42 (2011) 1648–1656 https://doi.org/10.1016/j.compositesb.2011.04.001.
[20] J.C. dos Santos, R.L. Siqueira, L.M.G. Vieira, R.T.S. Freire, V. Mano, T.H. Panzera, Effects of sodium carbonate on the performance of epoxy and polyester coir reinforced Composites, Polym. Test. 67 (2018) 533–544 https://doi.org/10.1016/j.polymertesting.2018.03.043.
[21] ASTM D3800-99, Standard Test Method for Density of High-Modulus Fibers, ASTM International, West Conshohocken, PA, 1999 https://www.astm.org/.
[22] T.H. Panzera, T. Jeannin, X. Gabrion, V. Placet, C. Remillat, I. Farrow, F. Scarpa, Static, fatigue and impact behaviour of an autoclaved flax fibre reinforced composite for aerospace engineering, Compos. Part B (2020) 1359–8368 https://doi.org/10.1016/j.compositesb.2020.108049.
[23] V. Weyenberg, J. Ivens, A. De Coster, B. Kino, E. Baetens, I. Verpoest, Influence of processing and chemical treatment of flax fibres on their composites, Compos. Sci. Technol. 63 (2003) 1241–1246 https://doi.org/10.1016/S0266-3538(03)00093-9.
[24] K.L. Pickering, M.G. Aruan Efendy, T.M. Le, A review of recent developments in natural fibre composites and their mechanical performance, Compos. Part A 83 (2016) 98–112 http://dx.doi.org/10.1016/j.compositesa.2015.08.038.
[25] SMITHS. 1200 Aluminium Technical Datasheet. https://www.smithmetal.com/pdf/aluminium/1xxx/1200.pdf. (Accessed 21 January 2020).
[26] MATWEB. Material property data. http://www.matweb.com/search/DataSheet.aspx?MatGUID=3f2253a553404b13893830617250b5d8&ckckr±=1.&ckck=1. (Accessed 26 March 2020).